U.Porto Journal of Engineering, 9:4 (2023) 109-124
ISSN 2183-6493
DOI: 10.24840/2183-6493_009-004_001945

Received: 25 November, 2022
Accepted: 4 May, 2023
Published: 22 September, 2023

# Dynamic effects on the lattice boom crane due to the wind, moving load and earthquake events

Luigi Solazzi[1], Nicola Danzi[2]
[1]Department of Mechanical and Industrial Engineering, University of Brescia, via Branze 38, 25123 BRESCIA, Italy (luigi.solazzi@unibs.it) ORCID 0000-0003-2265-9589
[2]Department of Mechanical and Industrial Engineering, University of Brescia, via Branze 38, 25123 BRESCIA, Italy (nicola.danzi@unibs.it) ORCID 0000-0001-5774-0833

**Abstract**
The present research concerns the evaluation of the dynamic effect on lattice boom cranes. The dynamic actions involved in this research are: wind, moving load and earthquake, assumed as time-varying actions. The research starts with the design of a large crane by adopting classical standards for these structures (UNI EN 13001 series). The elaborations were performed by analytical methods followed by solid model building and finite element analysis (Solidworks® and Ansys® software). The next step was to define the aforementioned loads acting on these structures.
The wind action model was compared with the static approach. Payload displacement induces high-intensity actions on the crane structure; to better understand these effects, several load curves were simulated. The last action considered is the earthquake phenomenon, which is not usually adopted to design this type of structure.

**Author Keywords.** Dynamic Effects, Wind Variable in Time, Moving Load, Earthquake Actions, Crane Design.

**Type:** Research Article
Open Access Peer Reviewed 

## 1. Introduction

Lifting equipment and, in general, cranes are machines that are subjected to many different loads. There are many standards that must be adopted for the design of the crane. Some of these standards are the EN 13001 series (EN 2021a), EN 15001(EN 2021b) and FEM 1.001 standards (FEM 1.001 1998). In general, these standards consider different load conditions due to the self-weight, the payload effect, the wind effect and so on, as constant actions that act on the crane structures. Nevertheless, these actions are not constant in time. These effects have been studied by Solazzi and Zrnic (2016); Gur and Ray-Chaudhuri (2013); (2014); Ambrosini, Riera, and Danesi (2002); Bošnjak, Zrnić, and Dragovic (2009); Chen et al. (2020). All these authors report the evaluation of different types of cranes subjected to variable wind actions. The main results related to the study of wind in a time-varying regime, are related to both intensity and vibration induced in the crane structures.

The 13001 series standards treat wind actions as a constant force applied to the entire lifting equipment. Because the force is constant, these standards do not include an analysis of time-varying wind force. These factors were introduced to supplement the standards by filling these gaps. In effect, different results are obtained from those that would be obtained by following the standards alone, since in this case the wind action is assumed to be a constant force over time. Time-varying actions are very dangerous because they can be the main causes of the collapse of structures (Kim et al. 2004; Klinger 2014; Frendo 2016; McCarthy, Soderberg, and

Dix 2009). The moving load or the crane components, in general, induce a dynamic effect that is related to several parameters. These parameters can be divided into two groups: (i) parameters that influence the stiffness of the structure and (ii) parameters that describe movement of the payload and of the crane itself. Solazzi et al. (2017) observed that, depending on the type of material and types of joints between the various elements that make up the entire structure, dynamic effects may be more or less amplified. On the other hand, Solazzi and Zrnic (2017) observed that the abrupt movement caused by the sudden release of the load causes an amplification of the dynamic effect, Solazzi, Remino, and Incerti (2019); Solazzi and Cima (2019); Zrnić et al. (2013); Yıldırım and Esim (2022) provide a clear example of amplification of the dynamic effect due to the application of the different laws of motion of the trolley and payload. All these studies were performed through analytical methods or numerical studies (by finite element method).

Seismic actions are types of actions that are not involved in the crane design process, but their intensity can be high enough (Wang et al. 2016; Solazzi 2011; Azeloglu, Kenan, and Edincliler 2021; Azeloglu, Edincliler, and Sagirli 2014) to cause the crane to collapse (*The 2011 Japan Earthquake and Tsunami: Reconstruction and Restoration* 2018). From a brief state of the art reported above, it is evident that dynamic actions are very important to define a correct and accurate factor of safety with respect to phenomena such as fatigue, buckling (local and global) and overturning moment, to which most cranes are subjected. The present research fits into this context with two objectives: the first is to study the effects of wind action, payload moving and seismic event on a lattice boom crane; the second concerns the understanding of how the contributions of the above-mentioned loads should be considered during the design phase and which of them cannot be neglected in any way.

## 2. Description of the crane studied

The container crane studied (lattice boom crane) consists mainly of two elements: a 70 m long liftable lattice boom and the 16 m high support structure that allows the boom to rotate around its axis. The load is applied at the end of the boom and is moved by lifting and rotating the boom. The boom is lifted by a system of ropes and pulleys (the minimum angle with respect to the horizontal plane is 21° while the maximum angle is 78° (Figure 1)); the boom rotation, on the other hand, is achieved by the rotation of the support structure. This type of crane is usually very large, so it is common to see that the boom is made with lattice structures, which minimizes both weight and wind forces while keeping the necessary stiffness. The following are the project specifications:

- liftable load with the boom in horizontal position: 40 tons;
- spreader weight: 15 tons;
- maximum outreach: 55 m;
- maximum height to take container: 35 m;
- maximum depth reached below the quay level: 15 m

Structural steel S355 (EN 10025) (steel alloy with $\sigma_{yield} = 355$ MPa; $\sigma_{ultimate} = 510$ MPa and elastic modulus $E = 206000$ MPa) was assumed for the construction of the crane. The main parameters assumed for the crane design are defined according to the EN 13001 series of standards (EN 2021a); in particular, the magnitude of maximum stresses, and thus, the factor of safety for static and fatigue phenomena, the stiffness of the structure, i.e., the maximum displacement, and local or global buckling phenomena were evaluated.

The FEM was composed of quadratic elements both for beam and solid elements. The entire model consists of about 2400 beam elements, representing the lattice boom, and 65000 solid elements, representing the support structure of the crane (the average size of the elements is approximately 100 mm). The analyses were performed on SolidWorks® and Ansys® software through the direct integration method. One of the most important parameters in dynamic analyses is the damping value. In these analyses, the value adopted for the Rayleigh damping is about 5% of the critical value, while $\alpha$ and $\beta$ were set to 1.5 and 0.001, respectively, for this type of structure (BROWNJOHN 1994; Carlotta Pagnini and Solari 2001; Rivin 2010; Luigi Solazzi and Zrnic 2017).

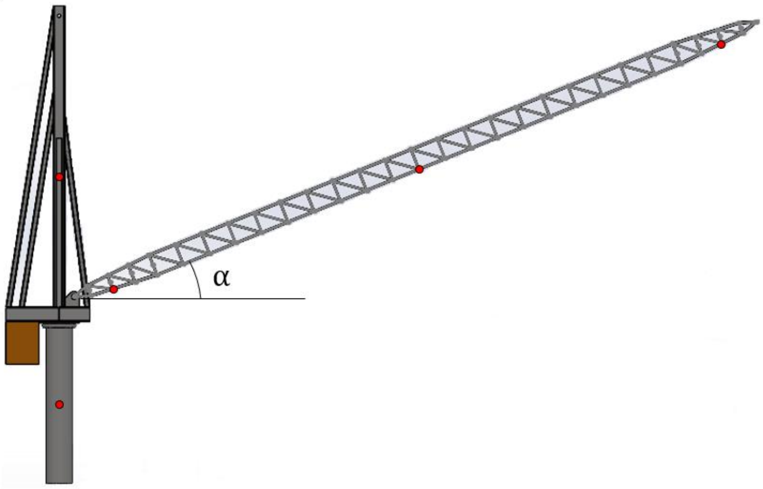


**Figure 1:** Representation of the angle of inclination of the boom

## 3. Static and buckling analysis results

The maximum crane displacement, due to payload in the lowered configuration, is approximately 320 mm, while in the raised configuration, is approximately 280 mm. From these numerical results, many considerations can be made. First of all, it is important to underline that the displacement of the crane in the different geometric configurations is coherent with what is defined in the standards. In fact, for example, the ratio between the length of the boom and its maximum displacement is of about 220 in the lowered configuration, while it is of about 250 in the raised one.

By solving the buckling problem, a vector of displacements, relative to the displacements of each individual node making up the mesh, of indefinite amplitude (defined minus a constant) was obtained. As a direct consequence, it was not possible to associate each mode with its maximum displacement. The coefficients that must be multiplied by the liftable load, to determine the critical loads, are shown in Table 1. The shape of the crane deformation corresponding to the first, i.e. the most critical, global buckling mode is ilustrated in.

| Mode | Lowered boom conf. | Raised boom conf. |
|---|---|---|
| 1 | 3.270 | 5.246 |
| 2 | 5.402 | 9.516 |
| 3 | 5.591 | 13.313 |
| 4 | 5.713 | 21.682 |
| 5 | 10.168 | 24.088 |
| 6 | 10.949 | 25.775 |
| 7 | 10.995 | 28.331 |
| 8 | 11.143 | 34.410 |
| 9 | 11.330 | 35.791 |
| 10 | 11.833 | 35.954 |

**Table 1:** Load factor for buckling phenomena for cranes in two different geometric configurations

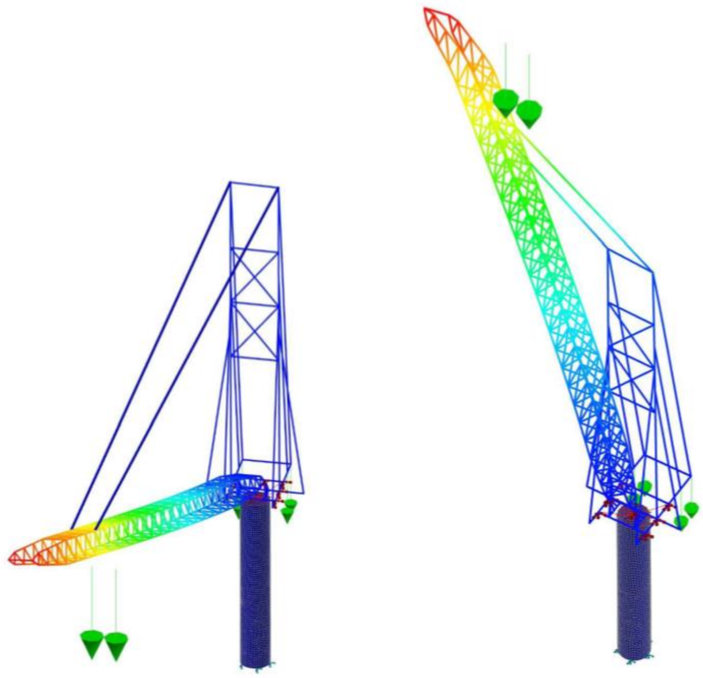

**Figure 2:** Crane deformation shape with respect to the first buckling mode in two different geometric configurations

## 4. Modal analysis results

Figure 3 shows the waveform of the main crane vibration modes for the lowered geometric configuration, while Figure 4 shows the same results in the raised configuration.

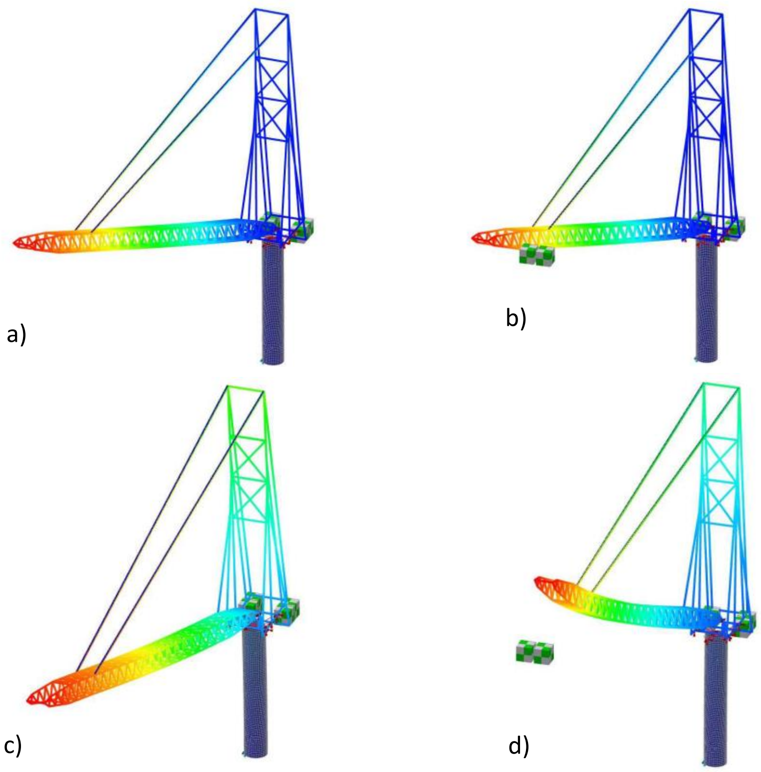

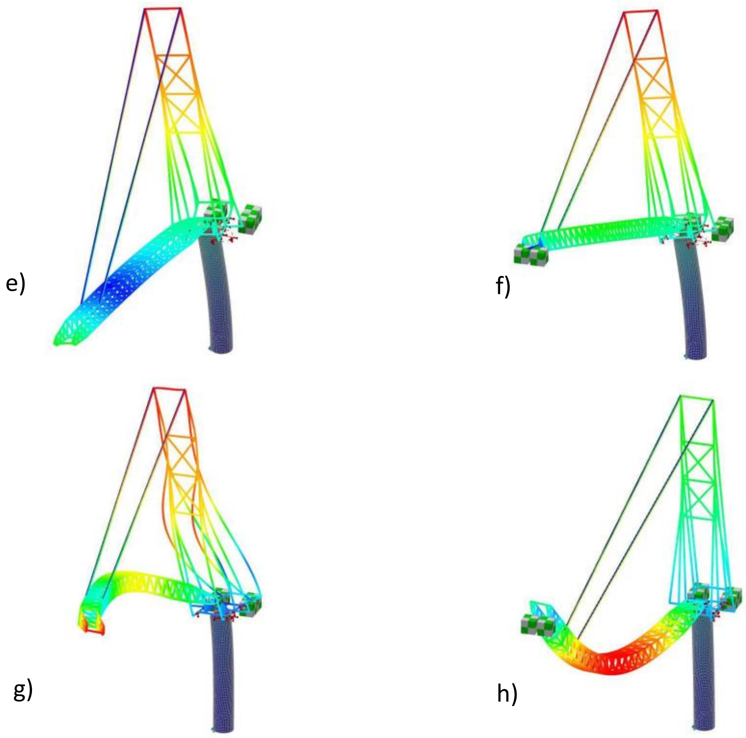


**Figure 3:** Crane waveforms corresponding to the first vibration modes in the lowered configuration: a) mode 1 without load; b) mode 1 with load; c) mode 2 without load; d) mode 2 with load; e) mode 3 without load; f) mode 3 with load; g) mode 4 without load; h) mode 4 with load

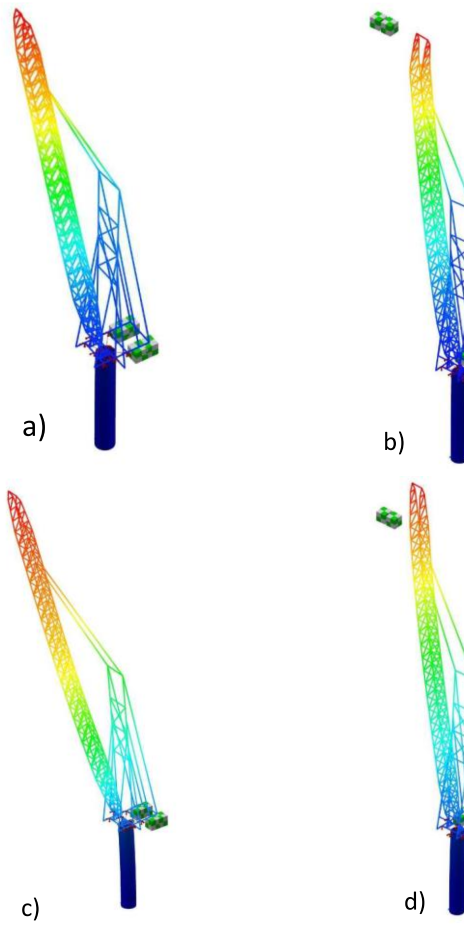

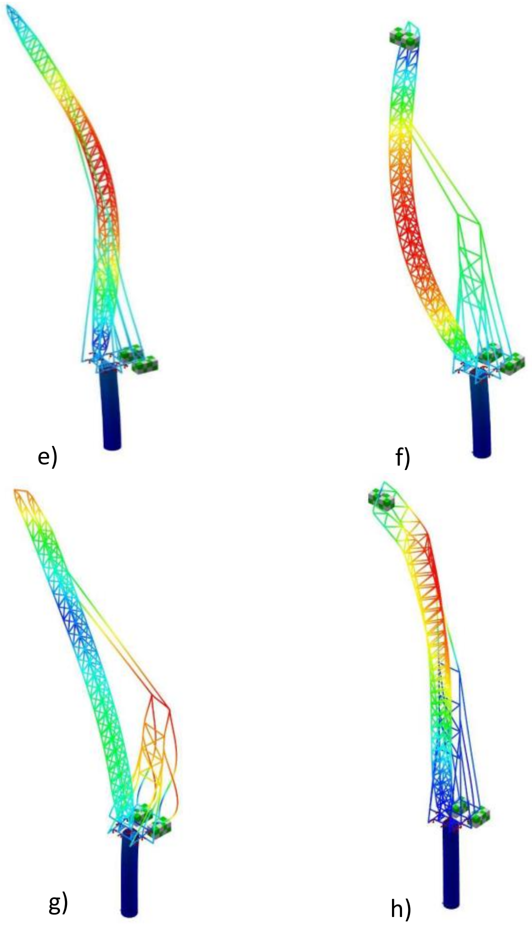


**Figure 4:** Crane waveforms corresponding to the first vibration modes in the raised configuration: a) mode 1 without load; b) mode 1 with load; c) mode 2 without load; d) mode 2 with load; e) mode 3 without load; f) mode 3 with load; g) mode 4 without load; h) mode 4 with load

Table 2 shows the values of the first ten vibration modes in two different geometric configurations, with and without the payload.

| | **Lowered boom configuration** | | **Raised boom configuration** | |
|---|---|---|---|---|
| **Mode** | **Without load** | **With load** | **Without load** | **With load** |
| 1 | 0.395 | 0.118 | 0.489 | 0.150 |
| 2 | 0.658 | 0.289 | 0.624 | 0.280 |
| 3 | 0.802 | 0.795 | 0.887 | 0.814 |
| 4 | 1.645 | 0.995 | 1.521 | 1.059 |
| 5 | 1.658 | 1.082 | 1.665 | 1.234 |
| 6 | 2.088 | 1.408 | 2.079 | 1.337 |
| 7 | 2.166 | 1.636 | 2.166 | 1.523 |
| 8 | 2.227 | 1.685 | 2.370 | 1.701 |
| 9 | 2.526 | 2.166 | 2.526 | 2.166 |
| 10 | 2.596 | 2.526 | 2.567 | 2.528 |

**Table 2:** Values of the first ten vibration modes [Hz]

As might be expected, the frequencies of each vibration mode changes if the crane lifts a load. Looking at Table 2, it can be seen that the presence of the load reduces the frequency of the respective vibration modes.

## 5. Wind effects

Aerodynamic wind actions can be divided into two components, one parallel to the incident wind direction (drag) and one orthogonal to it (lift) (Simiu and Yeo 2019; Holmes 2015). The magnitude can be evaluated through Formula (1) and (2).

$$F_D = \frac{1}{2}\rho[V(x,y,z,t)]^2 c_D A \tag{1}$$

$$F_L = \frac{1}{2}\rho[V(x,y,z,t)]^2 c_L A \tag{2}$$

Where $\rho$ is the air density; $V(x,y,z,t)$ is the field velocity; $c_L$ and $c_D$ represent lift and drag coefficients respectively and $A$ is the effective area involved.

Table 3 summarized the aerodynamic coefficients $c_D$ and $c_L$ for the crane boom and the support structure (Scarabino et al. 2005; Davenport and Riera 1998).

| | CD | CL |
|---|---|---|
| **Lowered crane boom** | 1.155 | 0.3 |
| **Raised crane boom** | 1.165 | 0.3 |
| **Strut** | 0.519 | 0.0 |
| **Pillar** | 1.455 | 0.3 |
| **External tie-road** | 1.779 | 0.0 |
| **Internal tie-road** | 1.525 | 0.3 |
| **Wind brace** | 1.359 | 0.3 |
| **Counterweight** | 1.335 | 0.3 |

**Table 3:** Drag and lift coefficients for the main parts of the crane

The wind actions implemented in this research are both constant and time-varying in order to emphasize the dynamic effects induced by the consideration of real situations.

In general, the wind velocity can be estimated by considering two different terms, the first constant in time and the second variable (Formula (3)).

$$V(x,y,z,t) = V_m(z) + v(x,y,t) \tag{3}$$

Where $V_m(z)$ is the mean wind speed at the height $z$, expressed by Formula (4), and $v(x,y,t)$ is the time-varying component, that is, the fluctuating wind speed.

$$V_m(z) = V_g \left(\frac{z}{Zg}\right)^{\alpha} \tag{4}$$

In Formula (4) $V_g$ represents the gradient wind velocity at gradient height $Zg$ (the height at which wind velocity becomes constant) and $\alpha$ is a power law index that depends on terrain conditions. $V_g$=20 m/s; $Zg$ =7.5 m; $\alpha$=1/7 are the parameters assumed in this research (Gur and Ray-Chaudhuri 2013; 2014). To study wind variability in time, it is possible to involve the power spectral density function. The most important are Kaimal and Van der Hoven models which are stationary stochastic methods.

By summarizing as much as possible what has been reported in Ambrosini, Riera, and Danesi (2002); Simiu and Yeo (2019); Davenport and Riera (1998); Tamura and Kareem (2013), both models assumed the same power spectral density function (Formula (5)), but with the Van der Hoven model, it is possible to obtain the wind speed fluctuation through the combination of the power spectral density, with the Formula (6) and (7). The fluctuating part from the Kaimal model can be obtained by Fast Fourier Transformation (FFT) (Formula (8)).

$$S_u(\omega, z) = \frac{1}{2}\frac{1}{2\cdot\pi}\cdot 200\cdot u(z_j)^2\cdot\frac{z_j}{V_m(z_j)}\cdot\frac{1}{\left[1+50\left(\frac{|\omega| z_j}{2\pi V_m(z_j)}\right)\right]^{\frac{5}{3}}} \tag{5}$$

$$A_i = \frac{2}{\pi}\cdot\sqrt{\frac{1}{2}[S_u(\omega_{i+1}) + S_u(\omega_i)]\cdot(\omega_{i+1}\cdot\omega_i)} \tag{6}$$

$$v(t) = \sum_{i=0}^{N} A_i\cdot cos(\omega_i + \varphi_i) \tag{7}$$

$$v\left(j, \frac{t}{\Delta t}\right) = Re\left[\sum_{k=0}^{j}\sum_{l=2}^{M} B(\omega, j, k)e^{ilp2\frac{\pi}{2N}}\right] \tag{8}$$

Where the principal parameters are: $A_i$ which represents the amplitude for each harmonic, $S_u(\omega_i)$ is the power spectral density for the angular frequency $\omega_i = 2\pi f_i$, while $v\left(j, \frac{t}{\Delta t}\right)$ represents the FFT required to simulate the fluctuating part of the wind speed (Gur and Ray-Chaudhuri 2013; 2014; Simiu and Yeo 2019).

For example, Figure 5 shows the wind speed versus time for three different points (defined in Figure 6) on the boom in the lowered configuration determined with the Kaimal model.

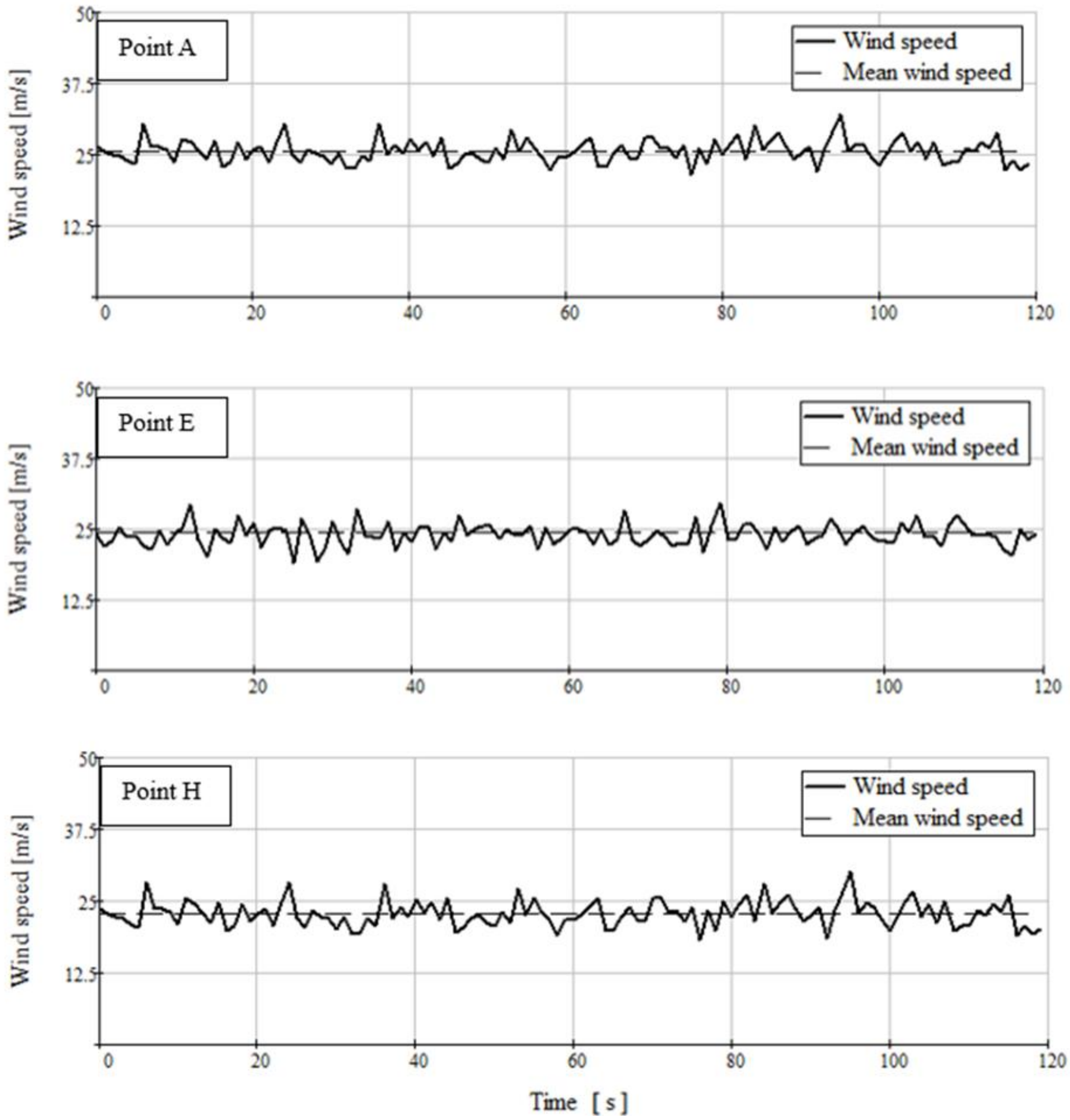


**Figure 5:** Wind speed trend (Kaimal model) for points A, E and H, shown in Figure 6 a), in the lowered configuration

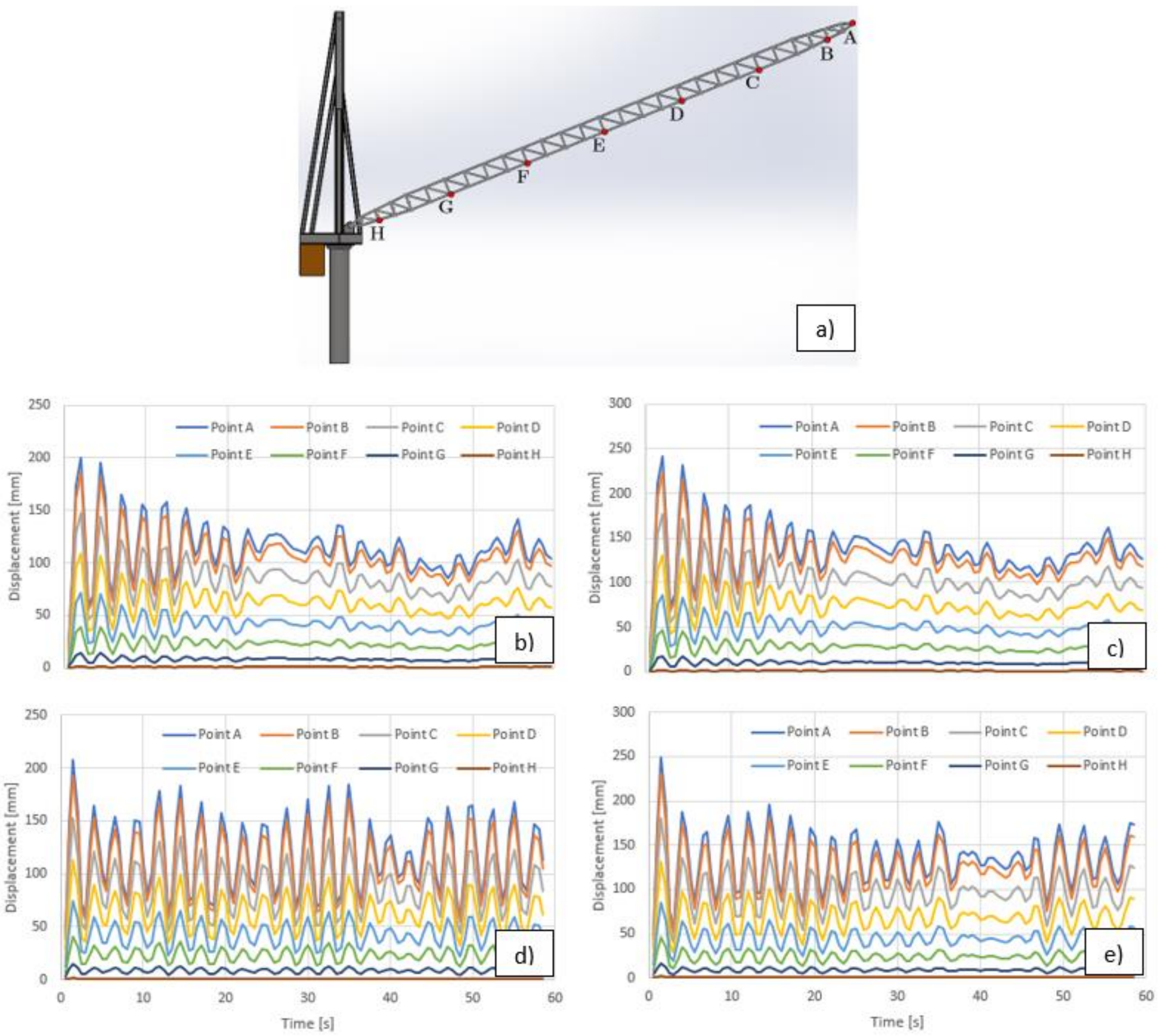


**Figure 6:** Displacement trend at different boom points in two different geometric configurations and two different stochastic models: a) important points on the boom; b) Van der Hoven model in lowered configuration; c) Van der Hoven model in raised configuration; d) Kaimal model in lowered configuration; e) Kaimal model in raised configuration

The maximum values of the displacement at the end of the boom are reported in Table 4, which are obtained by three different methods. In this table, “Const. Velocity” represents the constant wind speed condition, applied to the two crane configurations, and is equal to $V_m(z)$.

| | Van der Hoven model | Kaimal model | Const. Velocity |
|---|---|---|---|
| **Lowered configuration** | 200.6 | 207.8 | 77.9 |
| **Raised configuration** | 240.9 | 250.0 | 78.8 |

**Table 4:** Maximum displacement at the end of the boom [mm]

The effect of wind induces a crane displacement of a magnitude close to the one caused by the static effect of the payload. The most important factor is that the variable action shows a displacement that is about three times that estimated by applying constant speed to the crane. This result can be found for both implemented models based on power spectral density, particularly for the Van der Hoven and Kaimal models. The time-varying action shows another important aspect: variability induces stress cycles that cannot be neglected when assessing crane fatigue. For this observation, it is important to note that the Kaimal model generates displacement cycles with greater amplitude than the other model (Figure 6).

## 6. Moving load effects

The load can be applied to the crane with different laws affecting the entire handling system, such as the stiffness of the rope, the gearbox, the motor and its control with or without an inverter. To determine the influence of the load application law on the dynamic response of the crane, different formulations were considered; these are reported in Figure 7.

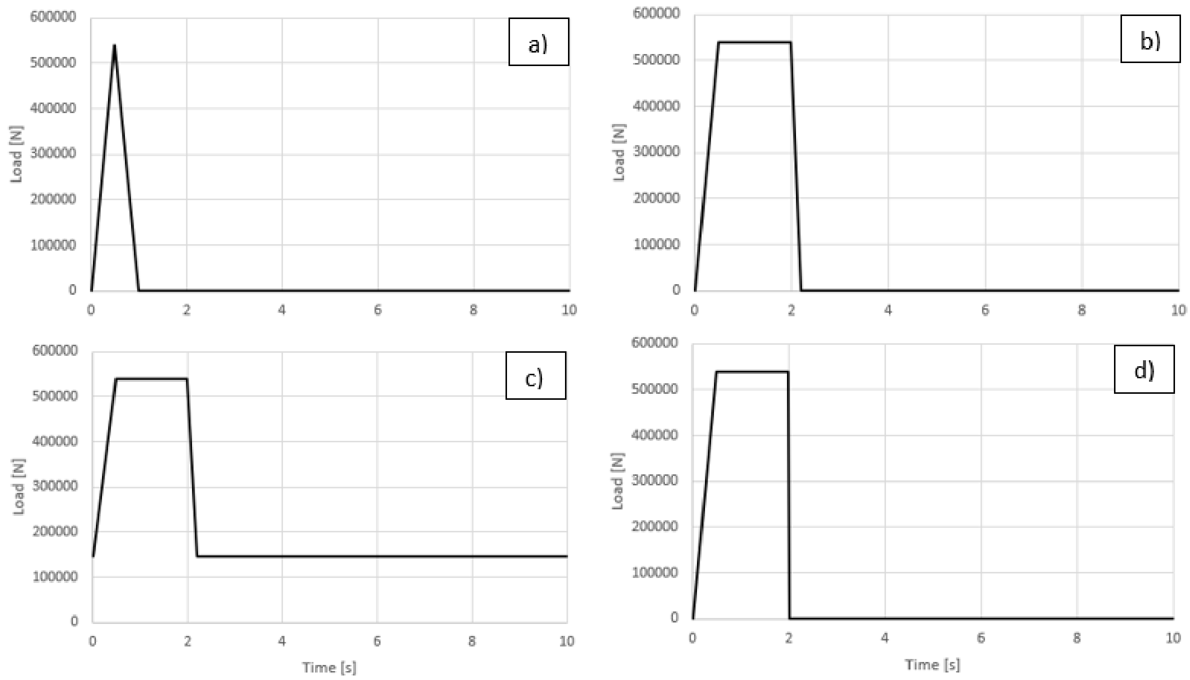


**Figure 7:** Different laws to load applied to the end boom crane: a) impulse; b) trapezoidal load 1; c) trapezoidal load 2; d) trapezoidal load 3

In particular, Figure 7 a) considers an impulsive force, Figure 7 b) and Figure 7 c) are similar, but in the last one only the payload has been removed; the spreader load remains on the crane. The last formulation (Figure 7 d) is related to the fact that, in case of sudden load release (like the breaking of the rope), there is a maximum backlash effect on crane structures.

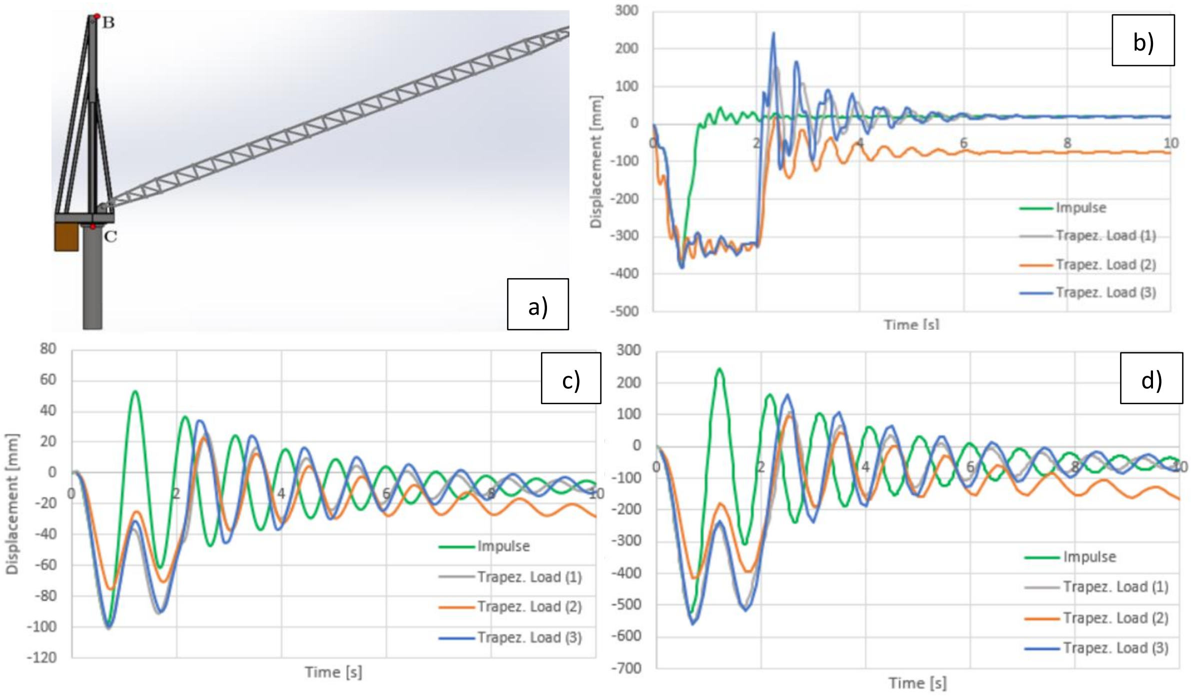


**Figure 8:** Displacement versus time for some points of the crane due to payload moving: a) important points on the boom; b) displacement at point A; c) displacement at point B; d) displacement at point C

Different moving load laws were applied to the crane. Through these analyses, it was possible to estimate the dynamic effect applied to the crane due to the moving load. In particular, in the payload application phase, the dynamic effect is about 1.25; this is in line with that defined by the standards. The most important is the dynamic effect induced by the abrupt release of the load; in this case, the magnitude of the backlash effect is very important and can cause the crane to collapse, like for example, due to buckling phenomena or overturning moment.

## 7. Earthquake actions effects

The earthquake actions are closely related to the site where the crane will be placed. Three different plausible spectra were adopted to study the seismic effects on the crane; each spectrum was characterized by the base accelerations. Figure 9 shows these spectra. According to various standards, in addition to the vertical action, the horizontal component in the two directions is also applied; in this case, the spectra were multiplied by the coefficient of 0.4.

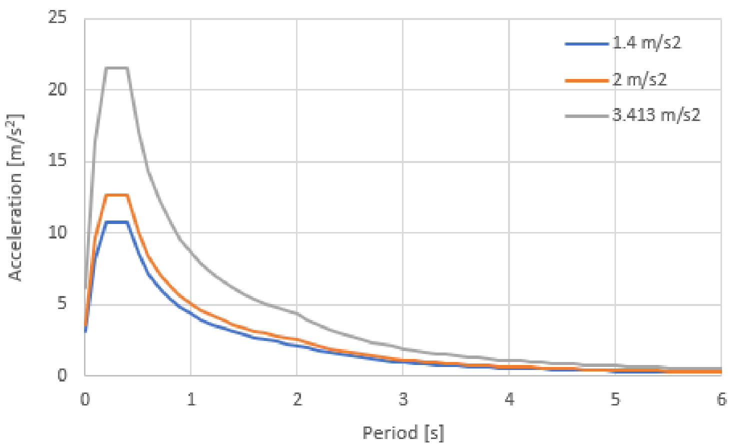


**Figure 9:** Accelerations of seismic spectra

Table 5 reports the maximum displacement for the end of the boom (point A in Figure 8) and structure (point B in Figure 8) concerning the three different spectra and with and without the load applied to it in the lowered geometric configuration. Table 6 is the same, but with the boom in a raised geometric configuration.

| | A=1.4 m/s$^2$ | | B=2.0 m/s$^2$ | | C=3.14 m/s$^2$ | |
|---|---|---|---|---|---|---|
| | Without load | With load | Without load | With load | Without load | With load |
| Point A_total displ. | 475.8 | 393.4 | 559.9 | 463.1 | 955.2 | 789.9 |
| Point A_X displacement | 130.7 | 107.1 | 153.8 | 126.0 | 262.3 | 214.9 |
| Point A_Y displacement | 280.5 | 228.2 | 330.1 | 268.5 | 563.3 | 458.0 |
| Point A_Z displacement | 365.9 | 305.8 | 430.5 | 360.1 | 734.5 | 614.2 |
| Point B | 230.7 | 224.6 | 271.4 | 264.3 | 463.1 | 451.0 |

**Table 5:**The boom in the lowered configuration, displacement in [mm]

| | A=1.4 m/s$^2$ | | B=2.0 m/s$^2$ | | C=3.14 m/s$^2$ | |
|---|---|---|---|---|---|---|
| | Without load | With load | Without load | With load | Without load | With load |
| Point A_total displ. | 582.2 | 372.3 | 685.0 | 483.3 | 1169.0 | 747.3 |
| Point A_X displacement | 395.8 | 154.8 | 465.8 | 182.1 | 794.5 | 310.8 |
| Point A_Y displacement | 102.4 | 41.5 | 120.5 | 48.9 | 205.6 | 83.4 |
| Point A_Z displacement | 418.4 | 337.2 | 492.2 | 396.9 | 839.8 | 677.2 |
| Point B | 222.3 | 189.3 | 261.5 | 222.8 | 446.2 | 380.1 |

**Table 6:**The boom in the raised configuration, displacement in [mm]

The crane displacement induced by the earthquake, correlated with the magnitude of the spectra, is very high compared to that obtained in static analyses. This effect makes very high stresses in the crane that can induce, for example, global and local buckling, plastic hinges and so on. The presence of the payload reduces the maximum displacement because the load reduces the natural frequencies of the crane, and thus, the effective seismic action on the crane is reduced. This consideration is true for both geometric configurations analyzed, i.e. lowered and raised.

## 8. Conclusions

This research reports the main numerical results performed on a specifically designed lattice boom crane to study the dynamic behavior of the crane subjected to different actions variable in time as wind (estimated through Van der Hoven and Kaimal models involving power spectral density functions), moving load considering different laws, and earthquake action considering three different spectra characterized by different base accelerations. The main conclusion is that dynamic action must always be involved in the crane design and verification process, because its intensity cannot be neglected at all. The response of the crane to the dynamic actions defined above generally shows greater displacement than that obtained from static analyses. The only exception is provided by the movement of the load, which causes a dynamic effect in line with the standards. On the other hand, the displacement induced by considering a time-varying wind is three times greater than that estimated by considering a constant wind action over time. Even considering the displacement induced by the earthquake action, it can be seen that they are greater than those calculated statically. The considerations were made by adopting only the displacement variable, but it is obvious that the magnitude of stresses, overturning moment, and so on, are closely related to the magnitude of displacement. In practice, if a constant wind speed is considered, displacements are underestimated, and consequently, the stresses, which are actually higher, are also underestimated. Through this study, it is clear that the standards do not allow for safe design. Research is still underway to extend this procedure to other types of cranes to see if this trend is confirmed also for other structures. In this way, it is intended to generalise the results obtained for this specific case to other types of structures, in order to suggest the implementation of the proposed approach as a complement for crane design.

**References**

Ambrosini, Ricardo Daniel, Jorge Daniel Riera, and Rodolfo Francisco Danesi. 2002. "Analysis of Structures Subjected to Random Wind Loading by Simulation in the Frequency Domain." *Probabilistic Engineering Mechanics* 17 (3): 233–39. https://doi.org/10.1016/S0266-8920(02)00008-5.

Azeloglu, C. Oktay, Ayse Edincliler, and Ahmet Sagirli. 2014. "Investigation of Seismic Behavior of Container Crane Structures by Shake Table Tests and Mathematical Modeling." *Shock and Vibration* 2014: 1–9. https://doi.org/10.1155/2014/682647.

Azeloglu, C. Oktay, Hamit Kenan, and Ayşe Edincliler. 2021. "Mathematical Modeling of Gantry Cranes under Seismic Excitation and Verification with Shake Table Tests." *Mechanics Based Design of Structures and Machines*, August, 1–12. https://doi.org/10.1080/15397734.2021.1967167.

Bošnjak, Srdan, Nenad Zrnić, and Branislaǘ Dragovic. 2009. "Dynamic Response of Mobile Elevating Work Platform under Wind Excitation." *Strojniski Vestnik/Journal of Mechanical Engineering* 55 (2).

BROWNJOHN, J M W. 1994. "ESTIMATION OF DAMPING IN SUSPENSION BRIDGES." *Proceedings of the Institution of Civil Engineers - Structures and Buildings* 104 (4): 401–15. https://doi.org/10.1680/istbu.1994.27199.

Carlotta Pagnini, Luisa, and Giovanni Solari. 2001. "Damping Measurements of Steel Poles and Tubular Towers." *Engineering Structures* 23 (9): 1085–95. https://doi.org/10.1016/S0141-0296(01)00011-6.

Chen, Wei, Xianrong Qin, Zhigang Yang, and Pengming Zhan. 2020. "Wind-Induced Tower Crane Vibration and Safety Evaluation." *Journal of Low Frequency Noise, Vibration and Active Control* 39 (2): 297–312. https://doi.org/10.1177/1461348419847306.

Davenport, A.G., and J.D. Riera. 1998. *Wind Effects on Building and Structures*. Taylor & Francis.

EN. 2021a. "Crane Safety - General Design - Part 2: Load Actions." EN 13001-2:2021.

EN. 2021b. "Cranes - Bridge and Gantry Cranes." EN 15011:2021.

FEM 1.001. 1998. "Rules for Design Hoisting Appliances." 1998 Edition.

Frendo, Francesco. 2016. "Gantry Crane Derailment and Collapse Induced by Wind Load." *Engineering Failure Analysis* 66. https://doi.org/10.1016/j.engfailanal.2016.05.008.

Gur, Sourav, and Samit Ray-Chaudhuri. 2013. "Probabilistic Assessment of Container Crane Under Wind Loading." In *Proceedings of the International Symposium on Engineering* *under Uncertainty: Safety Assessment and Management (ISEUSAM - 2012)*, 1049–60. India: Springer India. https://doi.org/10.1007/978-81-322-0757-3_72.

Gur, Sourav, and Samit Ray-Chaudhuri. 2014. "Vulnerability Assessment of Container Cranes under Stochastic Wind Loading." *Structure and Infrastructure Engineering* 10 (12): 1511–30. https://doi.org/10.1080/15732479.2013.834943.

Holmes, John D. 2015. *Wind Loading of Structures*. Taylor & Francis Group.

Kim, Dong Hyawn, Byung Cheol Oh, Sang Hun Han, Jae Seol Shim, In Sik Chun, Man Soon Song, and Ji Seong Jo. 2004. "Collapse of Container Cranes at Busan Ports under Typhoon Maemi." In *Proceedings of the International Offshore and Polar Engineering Conference*.

Klinger, C. 2014. "Failures of Cranes Due to Wind Induced Vibrations." *Engineering Failure Analysis* 43. https://doi.org/10.1016/j.engfailanal.2013.12.007.

McCarthy, Patrick, Erik Soderberg, and Anna Dix. 2009. "Wind Damage to Dockside Cranes: Recent Failures and Recommendations." In *TCLEE 2009: Lifeline Earthquake Engineering in a Multihazard Environment*. Vol. 357. https://doi.org/10.1061/41050(357)50.

Rivin, Eugene I. 2010. *Handbook on Stiffness and Damping in Mechanical Design*. ASME Press.

Scarabino, A., J. Marañón Di Leo, J. S. Delnero, and F. Bacchi. 2005. "Drag Coefficients and Strouhal Numbers of a Port Crane Boom Girder Section." *Journal of Wind Engineering and Industrial Aerodynamics* 93 (6). https://doi.org/10.1016/j.jweia.2005.03.004.

Simiu, Emil, and DongHun Yeo. 2019. *Wind Effects on Structures: Modern Structural Design for Wind*. 4th ed. Blackwell Pub.

Solazzi, L. 2011. "Ship to Shore Crane Subjected to Earthquake." *Procedia Engineering* 10: 2690–95. https://doi.org/10.1016/j.proeng.2011.04.448.

Solazzi, L, and M Cima. 2019. "Structural Dynamics of Big Gantry Crane Subjected to Different Trolley Move Laws." *Journal of Physics: Conference Series* 1264 (July): 012046. https://doi.org/10.1088/1742-6596/1264/1/012046.

Solazzi, L, C Remino, and G Incerti. 2019. "Overhead Crane Subjected to Impulse Loading." *Journal of Physics: Conference Series* 1264 (1): 012045. https://doi.org/10.1088/1742-6596/1264/1/012045.

Solazzi, Luigi. 2017. "Experimental and Analytical Study on Elevating Working Platform." *Procedia Engineering* 199: 2597–2602. https://doi.org/10.1016/j.proeng.2017.09.364.

Solazzi, Luigi, and Nenad Zrnic. 2016. "Numerical Study of Wind Actions Applied to a Low Profile Container Crane." *FME Transaction* 44 (1): 29–35. https://doi.org/10.5937/fmet1601029S.

Solazzi, Luigi, and Nenad Zrnic. 2017. "Design of a High Capacity Derrick Crane Considering the Effects Induced by Load Application and Release." *Istrazivanja i Projektovanja Za Privredu* 15 (1): 15–24. https://doi.org/10.5937/jaes15-11930.

Tamura, Yukio, and Ahsan Kareem, eds. 2013. *Advanced Structural Wind Engineering*. Tokyo: Springer Japan. https://doi.org/10.1007/978-4-431-54337-4.

*The 2011 Japan Earthquake and Tsunami: Reconstruction and Restoration*. 2018. Vol. 47. Cham: Springer International Publishing. https://doi.org/10.1007/978-3-319-58691-5.

Wang, Pingping, Lanfeng Yu, Wei Han, Hui Tang, Fei Yan, and Dengshan Zhao. 2016. "Analysis on Response of Tower Crane Structures under Random Earthquake Excitations." *Jixie Qiangdu/Journal of Mechanical Strength* 38 (1). https://doi.org/10.16579/j.issn.1001.9669.2016.01.036.

Yıldırım, Şahin, and Emir Esim. 2022. "Investigation of Dynamic Response of Multi- Carriages Double Bridge Overhead Type Crane System Subjected to the Moving Load." *Journal of the Brazilian Society of Mechanical Sciences and Engineering* 44 (3): 108. https://doi.org/10.1007/s40430-022-03419-9.

Zrnić, Nenad D., Vlada Gašić, Srdan Bošnjak, and Momčilo Dordević. 2013. "Moving Loads in Structural Dynamics of Cranes: Bridging the Gap between Theoretical and Practical Researches." *FME Transactions* 41 (4).